FEBS Letters 495 (2001) 52–55 FEBS 24795

Backbone dynamics of the channel-forming antibiotic zervamicin IIB studied by ^{15}N NMR relaxation

Dmitry M. Korzhnev[a,b], Eduard V. Bocharov[a], Anastasya V. Zhuravlyova[a], Vladislav Yu. Orekhov[b], Tatyana V. Ovchinnikova[a], Martin Billeter[b,c], Alexander S. Arseniev[a,*]

[a] *Shemyakin-Ovchinnikov Institute of Bioorganic Chemistry, Russian Academy of Sciences, ul. Miklukho-Maklaya 16/10, 117997 Moscow, Russia*
[b] *Swedish NMR Center at Göteborg University, P.O. Box 465, 405 30 Göteborg, Sweden*
[c] *Göteborg University, Lundberg Laboratory, Biochemistry and Biophysics, P.O. Box 462, 405 30 Göteborg, Sweden*

Received 15 February 2001; revised 6 March 2001; accepted 6 March 2001

First published online 3 April 2001

Edited by Thomas L. James

Abstract The backbone dynamics of the channel-forming peptide antibiotic zervamicin IIB (Zrv-IIB) in methanol were studied by ^{15}N nuclear magnetic resonance relaxation measurements at 11.7, 14.1 and 18.8 T magnetic fields. The anisotropic overall rotation of the peptide was characterized based on ^{15}N relaxation data and by hydrodynamic calculations. 'Model-free' analysis of the relaxation data showed that the peptide is fairly rigid on a sub-nanosecond time-scale. The residues from the polar side of Zrv-IIB helix are involved in micro–millisecond time-scale conformational exchange. The conformational exchange observed might indicate intramolecular processes or specific intermolecular interactions of potential relevance to Zrv-IIB ion channel formation. © 2001 Published by Elsevier Science B.V. on behalf of the Federation of European Biochemical Societies.

Key words: Peptaibol; Dynamics; Anisotropy; Model-free; Conformational exchange

1. Introduction

Zervamicin IIB (Zrv-IIB; Ac-Trp-Ile-Gln-Iva-Ile[5]-Thr-Aib-Leu-Aib-Hyp[10]-Gln-Aib-Hyp-Aib-Pro[15]-Phl; Aib – α-amino-isobutyric acid, Iva – D-isovaline, Hyp – 4-hydrohyproline, Phl – L-phenylalaninol) and several other zervamicins are representatives of the peptaibol family of peptide antibiotics produced by fungi [1–3]. Peptaibols are active against prokaryotic cells. Their toxic effect appears to be due to formation of ion channels that dramatically increase permeability of the cellular membrane. Peptaibols are rich of helix-promoting Aib residues, contain at least one Pro or Hyp residue and terminate with an amino alcohol.

The crystal structures of zervamicins and related peptides [4–7] and high-resolution nuclear magnetic resonance (NMR) structures of Zrv-IIB in mixed organic solvents [8] and in micellar environment (Shenkarev et al., to be published) have been determined. It was shown that Zrv-IIB adopts a conformation of a bent helix with a kink induced by Hyp10. The helix is essentially amphipathic. The polar side-chains of Gln3, Thr6, Hyp10, and Hyp13 form a polar surface on the convex side of the helix. Additionally, this polar face is enhanced by the exposed carbonyl oxygen of Aib7, the Gln11 side-chain and the C-terminal alcohol group of Phl16.

Zrv-IIB can form voltage-gated ion channels with multilevel conductance states in planar lipid bilayers and vesicular systems [9–11]. It is generally thought that the channel formation involves association of parallel helices surrounding an ion permeable pore within a lipid membrane [3,12,13]. The polar convex sides of the helices form the pore walls whereas the hydrophobic concave sides interact with hydrocarbon core of the membrane. Different conductance levels of the ion channel correspond to a different number of helices per bundle [9,10]. It is suggested that the helix bundle is stabilized by interactions between the polar side-chain groups of adjacent helices (see e.g. [13]).

To fully understand the mechanism of ion channel formation and its action, the data on the spatial structure of Zrv-IIB should be supplemented by information on the peptide intermolecular dynamics. The fact that Zrv-IIB maintains its well-defined spatial structure in organic solvents of different polarity and in micellar environment implies that the channel formation is not accompanied by substantial conformational changes [8]. However, the mobility of the polar side-chains of Zrv-IIB was suggested to be essential for ion transition through the channel and for adjustment of the monomer conformation upon the formation of the helix bundle [13]. Here we report the results of a ^{15}N–^{1}H NMR relaxation study of the backbone dynamics of Zrv-IIB solubilized in methanol. Potential relevance of the observed mobility to the formation of Zrv-IIB ion channel is discussed.

2. Materials and methods

2.1. ^{15}N relaxation measurements

The backbone ^{15}N longitudinal R_1 and transverse R_2 relaxation rates were measured on 11.7, 14.1 and 18.8 T Varian *Unity-Inova* spectrometers at 31°C; $^{15}N\{^{1}H\}$ nuclear Overhauser effects (NOEs) were measured at 11.7 and 14.1 T magnetic fields. The pulse sequences of Farrow et al. [14] were used. Temperature calibration and control in all experiments were carried out as described in Orekhov et al. [15]. The delay between consecutive scans in R_1 and R_2 experiments was set to 2 s. R_2 values were measured with 1.0 ms delay between the 180°

*Corresponding author. Fax: (7)-095-335 5033.
E-mail: aars@nmr.ru

Abbreviations: NMR, nuclear magnetic resonance; NOE, nuclear Overhauser effect; CPMG, Carr Pursell Meiboom Gill; CSA, chemical shift anisotropy; Zrv-IIB, zervamicin IIB

0014-5793/01/$20.00 © 2001 Published by Elsevier Science B.V. on behalf of the Federation of European Biochemical Societies.
PII: S0014-5793(01)02363-8

^{15}N pulses of the Carr Pursell Meiboom Gill (CPMG) sequence. The 90° ^{15}N pulse length never exceeded 40 μs, which allowed us to neglect off-resonance effects in R_2 (CPMG) measurements [16]. The values of ^{15}N{^{1}H} NOE were calculated as a ratio of signal intensities in spectra recorded with and without prior saturation of amide protons. The proton saturation in the NOE experiment was achieved by a sequence of 120° ^{1}H pulses applied during 4.0 s [17]. As a check if saturation transfer from the solvent to amide protons affects the ^{15}N{^{1}H} NOEs, the NOE experiment was repeated with 4.5 and 16.5 s delays between scans. Each of the R_1, R_2, and NOE measurements were repeated several times and the data were averaged over the measured data sets. To account for possible small systematic errors in the experimental data minimal uncertainties of 2% for R_1 and R_2 and ±0.1 for the NOE were assumed for the subsequent analysis.

2.2. 'Model-free' analysis of the relaxation data

The ^{15}N relaxation rates and ^{1}H{^{15}N} NOEs depend on the reorientation correlation function $C(t)$ for the corresponding NH vector [18]. $C(t)$ is given by the product of the correlation functions of overall rotation $C_O(t)$ and intramolecular motions $C_I(t)$ (see [19,20]). The transverse relaxation rate R_2 may also include a contribution R_{ex} due to conformational exchange on a micro–millisecond time-scale. Assuming particular forms for $C_O(t)$ and $C_I(t)$ one can extract their parameters and R_{ex} from the experimental relaxation data.

The relaxation data for Zrv-IIB were analyzed with the DASHA program [21] using different forms of $C_O(t)$ and $C_I(t)$ (Table 1). The parameters of $C_O(t)$ and $C_I(t)$, the contribution R_{ex} to R_2, assumed to be proportional to the square of the magnetic field, and the parameter uncertainties were obtained as described elsewhere (for a review see [20]). All calculations were performed with a NH distance of 0.102 nm. To account for the differences in individual ^{15}N chemical shift anisotropy (CSA) values the ^{15}N CSAs were considered to be adjustable parameters.

At the first preliminarily stage of data analysis the most complex form of $C_I(t)$ that appeared among individual NH groups of Zrv-IIB was determined. To do this each NH group was considered separately assuming different forms of $C_I(t)$ and isotropic $C_O(t)$ (Table 1). The relaxation data for different ^{15}N nuclei were analyzed with a rotation correlation time τ_R adjusted individually for each NH group [20,22] that allows the use of isotropic $C_O(t)$. The selection of an appropriated form of $C_I(t)$ was performed as described by Mandel et al. [23].

At the second stage the overall rotation of Zrv-IIB was characterized and the parameters of internal motions were refined. The most complex form of $C_I(t)$ anticipated at the first stage was used for all ^{15}N nuclei. The subsequent data analysis was carried out with different forms of $C_O(t)$ (Table 1). The parameters of molecular overall rotation were optimized simultaneously with the parameters of the internal motions for the set of NH groups of Zrv-IIB. Directions of the NH vectors in the molecular coordinate frame were taken from the NMR spatial structure of Zrv-IIB [8]. The selection of an appropriated form of $C_O(t)$ was performed and the quality of the data fitting was assessed using statistics criteria as described in [20].

2.3. Hydrodynamic calculations

The rotation diffusion tensor of Zrv-IIB was assessed by hydrodynamic calculations using the beads model approximation [20,21,24] based on the NMR structure of Zrv-IIB [8]. The calculations were performed with the DIFFC program [21]. Each residue of Zrv-IIB was represented by a bead of 3.5 Å radius centered at the position of its C^α atom.

3. Results and discussion

The relaxation rates and NOEs for ^{15}N nuclei of Zrv-IIB are shown in Fig. 1. The NOEs at 11.7 and 14.1 T are negative, indicating that reorientation of the NH groups occurs on a sub-nanosecond time-scale. The amide protons of the N-terminal Trp1, Ile2 (to a lesser extent) and Gln3 rapidly exchange with the solvent introducing considerable errors in ^{15}N{^{1}H} NOEs. For these NHs the NOEs measured with a 16.5 s delay between scans substantially exceed those obtained with a 4.5 s delay (Fig. 1c). Therefore, the results obtained here for N-terminal residues should be considered only qualitatively.

An important step in the analysis of ^{15}N relaxation data is the estimation of the overall rotation correlation time τ_R for isotropic molecules or the rotation diffusion tensor $\mathbf{D}_r$ for anisotropic molecules [20]. The parameters of molecular overall rotation derived from the relaxation data may be ambiguous since they are coupled with the particular form of $C_I(t)$ (Table 1) selected for polypeptide NH groups [20,25,26]. This ambiguity may be avoided if the most complex of the anticipated forms of $C_I(t)$ is selected for all ^{15}N nuclei [27]. Therefore, at a preliminary stage of the data analysis we determined the most complex form of $C_I(t)$ that appeared among NH groups of Zrv-IIB.

Preliminary analysis performed individually for each ^{15}N nucleus showed that Zrv-IIB exhibits heterogeneous internal motions. For several ^{15}N nuclei the analysis revealed conformational exchange on a micro–millisecond time-scale. The 'extended' form of $C_I(t)$ [28] (Table 1) implying intramolecular dynamics on two time-scales was not validated for any NH group. In the most complex case the data were accounted for by three adjustable parameters describing intramolecular motions – the order parameter S^2, the correlation time τ_e and the exchange contribution R_{ex} to R_2 at 11.7 T.

The overall rotation of Zrv-IIB was characterized based on the relaxation data for nine NH groups (all except NHs of the N-terminal Trp1–Gln3 and the C-terminal Phl16). The parameters of the overall rotation correlation function $C_O(t)$ (Table 1) were optimized together with the values describing individual NHs – S^2, τ_e, R_{ex} and ^{15}N CSA. This procedure allowed us to estimate the rotation diffusion tensor $\mathbf{D}_r$ for Zrv-IIB based on the relaxation data for a small set of ^{15}N nuclei exhibiting different types of intramolecular motions. Considering Zrv-IIB as an axially symmetric anisotropic molecule results in a statistically meaningful improvement of the data fitting with respect to the isotropic case. Transition to a more complex form of $C_O(t)$ accounting for diffusion of the asymmetric anisotropic molecule was not statistically vali-

Table 1
Correlation functions and their adjustable parameters

Type	Adjustable parameters	Reference	Description
$C_I(t)$	S^2, ($\tau_e \to 0$)	[19]	sub-picosecond internal dynamics
$C_I(t)$	S^2, τ_e	[19]	picosecond internal dynamics
$C_I(t)$	S_f^2, S_s^2, τ_s	[28]	dynamics on two time-scales: sub-picosecond and sub-nanosecond–nanosecond
$C_O(t)$	τ_R	[19]	isotropic overall rotation
$C_O(t)$	τ_R, $D_\parallel/D_\perp$, α, β	[31]	overall rotation of axially symmetric anisotropic molecule
$C_O(t)$	τ_R, D_z/D_x, D_z/D_y, α, β, γ	[31]	overall rotation of asymmetric anisotropic molecule

Here S, S_f, and S_s are order parameters of pico- and nanosecond time-scale motions, respectively; τ_e and τ_s are correlation times of pico- and nanosecond motions, respectively; D_i, $i = x, y, z$ are principal components of the rotational diffusion tensor $\mathbf{D}_r$ of the molecule; $D_\perp = D_x = D_y$ and $D_\parallel = D_z$; α, β, and γ are Euler angles defining the orientation of the molecular frame where $\mathbf{D}_r$ has a diagonal form with respect to the reference molecular frame. The effective overall rotation correlation time is defined as $\tau_R = (2(D_x+D_y+D_z))^{-1}$.

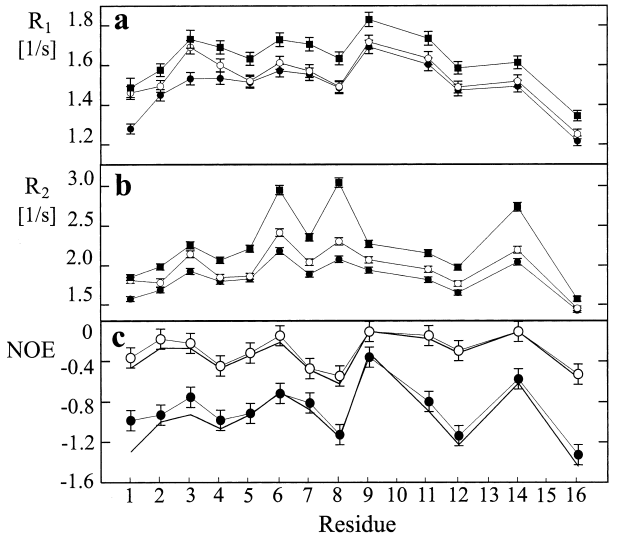

Fig. 1. Experimental relaxation data for the ^{15}N nuclei of Zrv-IIB measured at 11.7, 14.1 and 18.8 T spectrometers (filled circles, open circles, and filled squares, respectively): (a) R_1, (b) R_2, (c) $^{15}N\{^1H\}$ NOE. The NOE values obtained with 4.5 and 16.5 s delay between scans are drawn by bold and thin lines, respectively. The uncertainties shown for the relaxation data were used in the data analysis.

dated. The rotation diffusion tensor $\mathbf{D}_r$ derived from the relaxation data has a ratio of principal components $D_{\parallel}/D_{\perp}$ of 1.88 ± 0.35 and the principal axis directed along the helix. Tumbling of the peptide occurs on a sub-nanosecond time-scale with the effective $\tau_R = 0.75 \pm 0.06$ ns.

An axially symmetric prolate shape of Zrv-IIB, as revealed from the relaxation data, is in good correspondence with its spatial structure. The rotation diffusion tensor $\mathbf{D}_r$ obtained form hydrodynamic calculations has the ratios of principal components D_z/D_x and D_z/D_y of 2.76 and 2.77, respectively. The angle between symmetry axes of the rotational diffusion ellipsoids obtained from hydrodynamic calculations and from the relaxation data analysis is 25°. A somewhat lower degree of the rotational anisotropy obtained from the relaxation data could be accounted for by the solvent shell, which was disregarded in our hydrodynamic calculations, or by uncertainties arising due to the poor sampling of spatial directions by the small set of NH groups used in the relaxation data analysis.

The refined parameters describing internal motions of the NH groups of Zrv-IIB are shown in Fig. 2. The high mean order parameter $< S^2 > = 0.70 \pm 0.11$ suggests that the peptide is fairly rigid on a pico–sub-nanosecond time-scale (Fig. 2a). Order parameters are lowered for NHs of the N-terminal Trp1–Gln3 and the C-terminal Phl16, which might be explained by helix–coil transitions involving the helix ends (see e.g. [15,29]). The correlation times τ_e for most of the NHs from the central part of Zrv-IIB fall into a sub-picosecond time-scale (Fig. 2b). It should be noted that our analysis provides no information on nanosecond time-scale internal motions since these motions are effectively disguised by rapid overall rotation of Zrv-IIB. Pronounced contribution of R_{ex} to R_2 due to micro–millisecond time-scale conformational exchange was observed for the ^{15}N nuclei of Thr6, Leu8 and Aib14 (Fig. 2c). The contribution of R_{ex} to R_2 for the ^{15}N nuclei of Gln3, Ile5, and Aib7 is meaningful but less evident.

At a magnetic field of 18.8 T the variability of ^{15}N CSA at different sites of the peptide becomes of particular concern. Therefore, the relaxation data were analyzed with adjustable ^{15}N CSAs. Surprisingly, the observed mean ^{15}N CSA value of 193 ± 6 ppm (Fig. 2d) exceeds the values expected from solid-state NMR experiments or cross-correlated relaxation measurements (for a review see [20]) by more than 20 ppm. This could indirectly indicate some discord in the relaxation data measured at different fields. However, the use of a fixed CSA of 170 ppm for all ^{15}N nuclei of Zrv-IIB results in almost the same parameters as shown in Fig. 2a–c, but somewhat worsens the data fitting.

The conformational exchange on a micro–millisecond time-scale (Fig. 2d) involves mostly the species from the polar convex side of Zrv-IIB. The exchange was revealed for all NHs from the helix turn Ile5–Leu8. The highest R_{ex} was found for NH of Leu8 located in the same peptide plane with the solvent-exposed CO group of Aib7. This carbonyl oxygen was thought to provide the cation binding site within the ion pore [13]. Noticeable conformational exchange was also found for the NH groups of the polar residues Thr6 and Gln3 and for the NH of Aib14. The neighboring with Aib14 polar side-chain of Hyp13 was proposed to form a hydrogen bond with an adjacent monomer of the helix bundle [13]. The contacts between polar side-chains were proved to be essential for stabilization of the helix bundle when forming an ion channel [9]. The conformational changes upon formation of the helix bundle are likely to involve the polar species of Zrv-IIB. Thus, the micro–millisecond conformational exchange of the polar residues of Zrv-IIB might indicate an intramolecular mechanism for tuning the Zrv-IIB conforma-

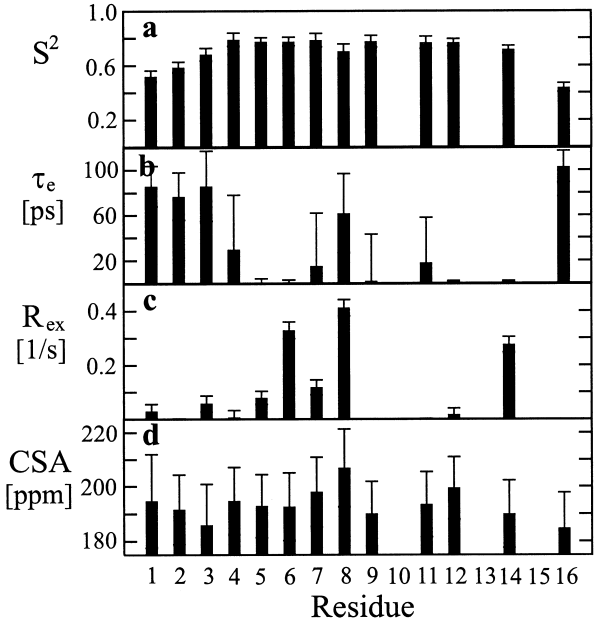

Fig. 2. Parameters of individual NH groups of Zrv-IIB obtained in 'model-free' analysis of the relaxation data and their uncertainties: (a) generalized order parameter S^2; (b) correlation time of picosecond time-scale internal motions τ_e; (c) exchange contribution R_{ex} to R_2 at 11.7 T; (d) ^{15}N CSA value. The parameters describing NHs of the residues 1–14 were optimized simultaneously with the parameters of $C_O(t)$ for an axially symmetric anisotropic molecule (Table 1). The parameters for NH groups of the N- and C-terminal residues 1–3 and 16 were calculated with fixed parameters of $C_O(t)$ using $\mathbf{D}_r$ obtained in the relaxation data analysis for the residues 4–14.

tion upon ion channel formation. Another possible explanation of the conformational exchange observed is the specific interactions between Zrv-IIB monomers as those reported for alameticin in the similar medium [30].

Acknowledgements: This work was supported by RFBR Grants 00-15-97877 and 00-04-48318 and a stipend from the Wenner-Gren Foundation to D.M.K. In part this work was supported by the Netherlands Organization for Scientific Research (NWO) Project 047.006.009 and by the Ministry of Industry, Science and Technology of Russian Federation. The experiments were performed at the Swedish NMR Centre. The authors are grateful to T.A. Balashova and Z.O. Shenkarev for helpful discussions and to J. Raap, D.A. Skladnev and E.V. Rogozhkina who provided us with the uniformly ^{15}N-labeled Zrv-IIB.

References

[1] Argoudelis, A.D., Dietz, A. and Johnson, L.E. (1974) 27, 321–328.
[2] Jen, W.C., Jones, G.A., Brewer, D., Parkinson, V.O. and Taylor, A. (1987) J. Appl. Bacteriol. 63, 293–298.
[3] Sansom, M.S.P. (1991) Prog. Biophys. Mol. Biol. 55, 139–235.
[4] Karle, I.L., Flippen-Anderson, J., Sukumar, M. and Balaram, P. (1987) Proc. Natl. Acad. Sci. USA 84, 5087–5091.
[5] Karle, I.L., Flippen-Anderson, J.L., Agarwalla, S. and Balaram, P. (1991) Proc. Natl. Acad. Sci. USA 88, 5307–5311.
[6] Karle, I.L., Flippen-Anderson, J.L., Agarwalla, S. and Balaram, P. (1994) Biopolymers 34, 721–735.
[7] Karle, I.L. (1996) Biopolymers 40, 157–180.
[8] Balashova, T.A., Shenkarev, Z.O., Tagaev, A.A., Ovchinnikova, T.V., Raap, J. and Arseniev, A.S. (2000) FEBS Lett. 466, 333–336.
[9] Agarwalla, S. et al. (1992) Biochem. Biophys. Res. Commun. 186, 8–15.
[10] Balaram, P., Krishna, K., Sukumar, M., Mellor, I.R. and Sansom, M.S.P. (1992) Eur. Biophys. J. Biophys. Lett. 21, 117–128.
[11] Kropacheva, T.N. and Raap, J. (1999) FEBS Lett. 460, 500–504.
[12] Fox, R.O. and Richards, F.M. (1982) Nature 300, 325–330.
[13] Sansom, M.S.P., Balaram, P. and Karle, I.L. (1993) Eur. Biophys. J. Biophys. Lett. 21, 369–383.
[14] Farrow, N.A. et al. (1994) Biochemistry 33, 5984–6003.
[15] Orekhov, V.Y., Korzhnev, D.M., Diercks, T., Kessler, H. and Arseniev, A.S. (1999) J. Biomol. NMR 14, 345–356.
[16] Korzhnev, D.M., Tischenko, E.V. and Arseniev, A.S. (2000) J. Biomol. NMR 17, 231–237.
[17] Markley, J.L., Horsley, W.J. and Klein, M.P. (1971) J. Chem. Phys. 55, 3604.
[18] Abragam, A. (1961) The Principles of Nuclear Magnetism, Clarendon Press, Oxford.
[19] Lipari, G. and Szabo, A. (1982) J. Am. Chem. Soc. 104, 4546–4559.
[20] Korzhnev, D.M., Billeter, M., Arseniev, A.S. and Orekhov, V.Y. (2001) Prog. Nucl. Magn. Reson. Spectrosc. 38, 197–266.
[21] Orekhov, V.Y., Nolde, D.E., Golovanov, A.P., Korzhnev, D.M. and Arseniev, A.S. (1995) Appl. Magn. Reson. 9, 581–588.
[22] Schurr, J.M., Babcock, H.P. and Fujimoto, B.S. (1994) J. Magn. Reson. Ser. B 105, 211–224.
[23] Mandel, A.M., Akke, M. and Palmer, A.G. (1996) Biochemistry 35, 16009–16023.
[24] de la Torre, J.G. and Bloomfield, V.A. (1981) Q. Rev. Biophys. 14, 81–139.
[25] Orekhov, V.Y., Pervushin, K.V., Korzhnev, D.M. and Arseniev, A.S. (1995) J. Biomol. NMR 6, 113–122.
[26] Korzhnev, D.M., Orekhov, V.Y. and Arseniev, A.S. (1997) J. Magn. Reson. 127, 184–191.
[27] Andrec, M., Montelione, G.T. and Levy, R.M. (1999) J. Magn. Reson. 139, 408–421.
[28] Clore, G.M., Szabo, A., Bax, A., Kay, L.E., Driscoll, P.C. and Gronenborn, A.M. (1990) J. Am. Chem. Soc. 112, 4989–4991.
[29] Korzhnev, D.M., Orekhov, V.Y. and Arseniev, A.S. (1999) J. Biomol. NMR 14, 357–368.
[30] North, C.L., Franklin, J.C., Bryant, R.G. and Cafiso, D.S. (1994) Biophys. J. 67, 1861–1866.
[31] Woessner, D.E. (1962) J. Chem. Phys. 37, 647–654.